Total cross-sections for positron and electron scattering from α-tetrahydrofurfuryl alcohol

2011 New J. Phys. 13 063019

(http://iopscience.iop.org/1367-2630/13/6/063019)

New Journal of Physics
The open-access journal for physics

Total cross-sections for positron and electron scattering from α-tetrahydrofurfuryl alcohol

A Zecca[1], L Chiari[1,2], G García[3], F Blanco[4], E Trainotti[1] and M J Brunger[2,5,6]

[1] Department of Physics, University of Trento, Povo, I-38123 Trento, Italy
[2] ARC Centre for Antimatter-Matter Studies, School of Chemical and Physical Sciences, Flinders University, GPO Box 2100, Adelaide, South Australia 5001, Australia
[3] Instituto de Matemáticas y Física Fundamental, Consejo Superior de Investigaciones Cientificas, Serrano 121, 28006 Madrid, Spain
[4] Departamento de Física Atómica, Molecular y Nuclear, Facultad de Ciencias Físicas, Universidad Complutense, Avda. Complutense s/n, E-28040 Madrid, Spain
[5] Institute of Mathematical Sciences, University of Malaya, 50603 Kuala Lumpur, Malaysia
E-mail: michael.brunger@flinders.edu.au

New Journal of Physics **13** (2011) 063019 (11pp)
Received 30 March 2011
Published 10 June 2011
Online at http://www.njp.org/
doi:10.1088/1367-2630/13/6/063019

Abstract. In this paper, we report original measurements of total cross-sections (TCSs) for positron scattering from an important biomolecule, α-tetrahydrofurfuryl alcohol (THFA). The energy range of these measurements was 0.15–50.15 eV, whereas the energy resolution was ~260 meV. In addition, we report theoretical results, calculated within the independent-screened additivity rule (IAM-SCAR) formalism, on the corresponding electron impact total cross-sections. In this case, the energy range is 1–10 000 eV. With the advent of new particle track simulation codes, which incorporate accurate atomic and molecular data in order to provide interaction details at the nanoscale, interest in positron and electron TCSs has enjoyed something of a recent renaissance as they specify the mean free path between collisions in such codes. Because the present data are, to the best of our knowledge, the first TCSs to be reported for positron scattering from THFA, they fill an important void in the knowledge available to us from the literature.

[6] Author to whom any correspondence should be addressed.

Contents

1. Introduction

Further developments in the biomedical uses of radiation are necessitating an increased level of detail, in order to understand the interaction processes initiating radiation damage in matter. In particular, reduced volume irradiation techniques such as brachytherapy [1], in which radiation emitters are placed close to the target, require not only traditional dosimetric methods to prescribe the treatment, but also an evaluation of possible side effects in the surrounding sensitive areas. This need to describe radiation effects at the molecular level has led to the development of the concept of nanodosimetry, namely a procedure for quantifying radiation damage in nanovolumes. Absorbed dose is probably not a proper quantity to characterize the effects at the nanoscale; rather, a detailed description of the interaction processes occurring in a nanosize target and their implications in terms of radiation damage is what is really required. As this nanoregion of interest could be relatively far (approximately microns to even millimetres) from the original track of the incident high-energy primary particles, be they photons, electrons or positrons (such as in positron emission tomography), an accurate description of single tracks of secondary particles will be essential for that purpose. These reasons have motivated the development of a new low-energy particle track simulation (LEPTS) code [2], specifically designed to provide interaction details at the nanoscale. This simulation procedure is based on a step-by-step Monte Carlo code, which uses as input parameters the experimental and theoretical electron and positron scattering cross-sections, including total cross-sections (TCSs), and energy loss distribution functions. Hence, one of the aims of this paper is to provide an important subset of such data for use in such simulations. Note that in any modelling of PET, both positron and electron TCSs will be required, as the incident high-energy positrons will produce secondary electrons through ionization.

α-tetrahydrofurfuryl alcohol (THFA; $C_5H_{10}O_2$) is an aromatic compound whose molecular structure is schematically represented in figure 1. As specifically demonstrated in the paper by Milosavljević *et al* [3], the structure of THFA is very similar to that of 2-deoxy-D-ribose (deoxyribose) and is thus considered a model compound to investigate the collision of positrons and electron with biomolecules. THFA also possesses several physico-chemical properties that render it interesting to study from a fundamental perspective. These include that its electron charge cloud has quite a significant spatial extent (dipole polarizability, $\alpha = 70.18$ au [4]) and that it has a relatively strong permanent dipole moment ($\mu \sim 2$ D [5]). We have previously seen for both positrons (e.g. [6]) and electrons (e.g. [7]) that such target molecular properties can have an important impact on the scattering dynamics of the system under study. This point will be addressed again later in our discussion.

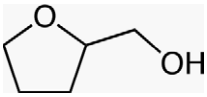

Figure 1. Schematic diagram of the THFA molecule.

To the best of our knowledge there have been no previous studies of positron scattering from THFA. The situation with respect to electron scattering is, however, a little better. In this regard, we mention that the total cross-section measurements of Możejko *et al* [5] for energies from 1 to 370 eV and the elastic differential cross-section (DCS) measurements of Milosavljević *et al* [3] for energies from 40 to 300 eV and scattered electron angles of 30°–110°. A preliminary IAM with screened additivity rule (AR) correction calculation was also reported as a part of the latter study [3]. However, that theoretical work did not satisfy the optical theorem (see later), so it can be considered as superseded by the present study. In addition, it did not include rotational excitation, which is a feature of the present computation.

In the next section, we give a summary of our experimental apparatus and techniques, followed by details of our calculations. In section 4, we report the present results and a discussion of these results, before drawing some conclusions from our investigation.

2. Experimental details

The Trento University spectrometer was developed by Zecca and has been described previously many times (see e.g. [8–13]). We therefore do not repeat the details here, except for noting that a tungsten moderator of thickness 1 μm [14] was employed in conjunction with a radioactive ^{22}Na isotope (current activity $\sim$1.6 mCi) and some electrostatic optics in order to produce the positron beam. Note that it is standard practice in our laboratory, as a check for the validity of our techniques and procedures, to carry out preliminary validation measurements using targets for which the positron scattering total cross-sections are considered to be well known. Such 'benchmarked' systems might be drawn from the lighter rare gases [15], for example, or from molecular nitrogen.

The basis of all our linear transmission experiments is the Beer–Lambert law, as defined by

$$I_1 = I_0 \exp\left(\frac{-(P_1 - P_0)L\sigma}{kT}\right), \tag{1}$$

where I_1 is the positron beam count rate at pressure P_1, the target pressure being measured with the THFA routed to the scattering cell, k is the Boltzmann constant (1.38×10^{-23} JK^{-1}) and T is the temperature of the THFA vapour (K), as accurately measured by using a calibrated platinum (PT100) resistance thermometer that is in excellent thermal contact with the scattering chamber. In our geometry, gas molecules thermalize with the scattering cell walls; therefore, the scattering chamber temperature can be considered a good approximation of the gas temperature. σ is the TCS of interest at a given incident positron energy; I_0 is the positron count rate at P_0, the pressure with the THFA diverted into the vacuum chamber, i.e. away from the scattering cell; and L is the length of the scattering region.

For a physical application of equation (1), several crucial precautions should be taken and care must be exercised during the measurements. These considerations include minimizing the

double-scattering events and ensuring that the TCSs are independent of pressure. In addition, only a high-purity THFA sample (∼99%) was used (Sigma–Aldrich). Note that while THFA is a liquid at room temperatures, it is sufficiently volatile to enable us to carry out our measurements. Our sample holder was also thermally insulated in order to ameliorate for any possible effects caused by any room temperature fluctuations. Such fluctuations were, however, typically small. Further note that to minimize any possible impurities affecting our measurements, freeze-pump-thaw cycles were employed here.

The geometrical length of the scattering region is 22.1 ± 0.1 mm, with apertures of 1.5 mm diameter at both the entrance and exit of the scattering cell. End effects were minimized in this study by having equal and relatively small diameter entrance and exit apertures in the scattering cell. As a consequence, we believe their contribution to the uncertainty in the value of L is likely to be less than 0.2%. In our application of equation (1), the value of L used is always corrected to account for the path increase caused by the gyration of the positrons in the focusing axial magnetic field present in the scattering region. For incident positron energies up to 30.15 eV, $B \sim 11$ G and the value of L increased by ∼5.5%, whereas for energy values between 32.65 and 50.15 eV, $B \sim 4$ G, leading to an increase in L of ∼2%. From a consideration of the size of the entrance and exit apertures of our scattering cell, and their separation, the angular acceptance ($\Delta\theta$) of the Trento spectrometer is $\approx 4^\circ$, which compares favourably with those from the Yamaguchi spectrometer [16] ($\Delta\theta \approx 7^\circ$) and the Detroit apparatus [17] ($\Delta\theta \approx 16^\circ$). The gyration of the positrons can also potentially increase the angular resolution error compared with the no-field case [18]. Using some of the analytic formulae detailed in Kauppila *et al* [17], but for the typical experimental conditions of our measurements, estimates of the energy-dependent angular discrimination could be obtained. We found that they varied from $\sim 17^\circ$ at 1 eV positron energy to $\sim 5.4^\circ$ at 10 eV. This can also be corrected for, provided appropriate absolute elastic DCSs (theory or experimental) are available [19]. Unfortunately, such positron–THFA DCSs are currently unknown, so the TCSs we report here represent a lower bound on the exact values.

It is crucial that the energy scale be calibrated accurately. The zero for the energy scale, in the absence of the target gas, was determined in this investigation using a retarding potential analysis of the positron beam [20]. We now believe that the error in our energy scale is of ±0.1 eV. Measurements carried out during the last four–five years show a surprising stability in the energy zero (variance < 0.05 eV) when using the tungsten moderator. The same measurements allow us to evaluate an energy width of the positron beam of ∼260 meV, with an uncertainty on this determination of at most ±50 meV. Note that this resolution was achieved due to an additional monochromation of the positron beam from a hemispherical deflector incorporated into the spectrometer design. It is also very important to accurately measure the scattering cell pressure, which we achieve with an MKS 627B capacitance manometer operated at 45 °C. As the manometer temperature was different from that for the target gas in the scattering cell, thermal transpiration corrections to the pressure readings are made using the model of Takaishi and Sensui [21]. Typically, this led to a maximum correction on the TCS of +3%. One final caveat on the data we report here should be noted. All the experimental data are convoluted with the finite energy resolution of our positron beam, although the effect of this on the measured TCSs is most manifest at positron energies below ∼0.5 eV, which coincides with the energies where the slope of the TCS as a function of energy is also greatest. In practice, this physically implies that, when corrected for this effect, our lowest-energy TCSs should be somewhat higher in magnitude than we present here.

Table 1. The present TCSs ($\times 10^{-20}$ m^2) for positron scattering from THFA ($C_5H_{10}O_2$).

Energy (eV)	TCS (10^{-20} m^2)	TCS error (10^{-20} m^2) ($\pm 1\sigma$)	Energy (eV)	TCS (10^{-20} m^2)	TCS error (10^{-20} m^2) ($\pm 1\sigma$)
0.15	280.62	5.68	4.15	42.45	2.60
0.16	261.61	19.45	5.15	39.34	1.40
0.20	258.94	2.61	6.15	35.49	1.36
0.25	214.31	23.57	7.15	33.35	1.41
0.30	186.41	13.29	8.15	32.06	0.96
0.35	196.68	16.04	9.15	31.62	0.73
0.45	157.85	12.95	10.15	31.21	1.04
0.55	142.44	12.89	12.15	29.57	1.34
0.65	135.20	13.38	15.15	29.66	2.20
0.75	120.29	3.07	17.65	30.04	0.84
0.85	108.95	9.58	20.15	28.88	1.07
0.95	102.69	5.43	22.65	28.78	0.95
1.05	91.64	4.52	25.15	28.18	1.00
1.15	91.92	8.81	27.65	27.63	1.31
1.40	79.74	5.57	30.15	27.98	3.24
1.65	74.16	2.32	32.65	26.47	1.56
1.85	69.37	3.43	35.15	29.16	1.74
2.15	63.50	4.53	40.15	28.90	2.25
2.65	54.23	1.97	45.15	29.02	1.93
3.15	46.41	1.66	50.15	28.78	0.74

Finally, we note that the data collection and analysis codes were driven by software developed at the University of Trento, for application on a personal computer. The positron energy range of the present TCS measurements was 0.15–50.15 eV, with the overall errors on our total cross-sections estimated as being within the 5–15% range. Note that the overall errors are formed from the quadrature sum of quantities such as the statistical uncertainties on our data (see table 1), the uncertainty in our thermal transpiration corrections, the uncertainty in the value of L and the uncertainty in the absolute pressure readings ($\sim$0.3%), as per the manufacturer's specifications. All our measurements were taken under stable positron beam conditions.

3. Theoretical details

The first subjects of the present calculations are the atoms constituting THFA, namely C, O and H. We represent each atomic target by an interacting complex potential (i.e. the optical potential), whose real part accounts for the elastic scattering of the incident electrons, while the imaginary part represents the inelastic processes that are considered as 'absorption' from the incident beam. To construct this complex potential for each atom, the real part of the potential is represented by the sum of three terms: (i) a static term derived from a Hartree–Fock calculation of the atomic charge distribution [22], (ii) an exchange term

to account for the indistinguishability of the incident and target electrons [23] and (iii) a polarization term [24] for the long-range interactions which depend on the target dipole polarizability (α). The imaginary part, following the procedure of Staszewska *et al* [25], then treats inelastic scattering as electron–electron collisions. However, we initially found some major discrepancies in the available atomic scattering data, which were subsequently corrected when a physical formulation of the absorption potential [26] was introduced. Further improvements to the original formulation [25], such as the inclusion of screening effects, local velocity corrections and in the description of the electron's indistinguishability [27], finally led to a model that provides a good approximation of electron–atom scattering over a broad energy range [28].

To calculate the cross-sections for electron scattering from THFA, we follow the independent atom method (IAM) by applying what is commonly known as the additivity rule (AR). In this approach, the molecular scattering amplitude is derived from the sum of all the relevant atomic amplitudes, including the phase coefficients, which leads to the molecular DCSs for the molecule in question. Integral cross-sections (ICSs) can then be determined by integrating those DCSs, with the sum of the elastic ICS and the absorption ICS (for all inelastic processes except rotations and vibrations) then giving the TCSs. Alternatively, the ICSs for THFA can also be derived from the relevant atomic ICSs in conjunction with the optical theorem [27]. Unfortunately, in its original form, we found an inherent contradiction between the ICSs derived from those two approaches, which suggested that the optical theorem was being violated [29]. As a consequence, our preliminary electron–THFA [3] calculations are likely to suffer from this problem so that the current results supersede (and extend) those original computations. This difficulty, however, has now been solved [29] by employing a normalization procedure during the computation of the DCSs, so that the ICSs derived from the two approaches are now entirely consistent [29]. A limitation of the AR is that no molecular structure is considered, so that it is really only applicable when the incident electrons are so fast that they effectively see the target molecule as a sum of the individual atoms (typically above $\sim$100 eV). To reduce this limitation, Garcia and colleagues [30, 31] introduced the screened additivity rule (SCAR) method, which considers the geometry of a relevant molecule (atomic positions and bond lengths) by using some screening coefficients. With this correction the range of validity might be extended to incident electron energies of 50 eV or a little lower. Furthermore, for polar molecules such as THFA ($\mu \sim 2$ D [5]), additional dipole-excitation cross-sections can be calculated to further extend the range of validity ($\sim$20 eV). In the present implementation, rotational excitation cross-sections for a free electric dipole are calculated by assuming that the energy transferred is low enough, in comparison with the incident energy, to validate the first Born approximation. Under these circumstances, we have calculated a rotational excitation cross-section for $J \rightarrow J'$ for THFA at 300 K by weighting the population for the Jth rotational quantum number at that temperature and estimating the average excitation energy from the corresponding rotational constants. The most important effect of this latter correction is a significant increase in the absolute value of the cross-section (see figure 2) at the lower incident electron energies. Note, finally, that the IAM-SCAR + rotations method also includes a procedure where interference terms were normalized (reduced) as much as necessary to ensure that the integrated elastic values also satisfied the (corrected) AR.

We are currently trying to extend our methodology to also calculate positron scattering cross-sections. At the moment, however, the treatment for the positronium formation channel is proving to be somewhat problematic.

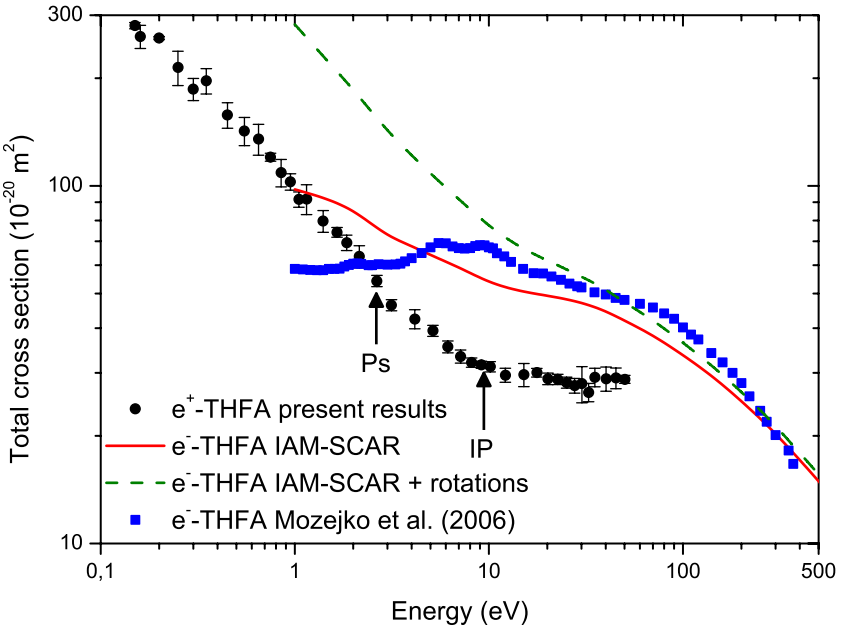

Figure 2. TCSs ($\times 10^{-20}$ m^2) for positron scattering from THFA. The present data are denoted by (•). The positronium formation threshold and the first ionization potential are indicated by arrows labelled 'Ps' and 'IP'. Also plotted are our electron scattering TCSs within the IAM-SCAR (——) and IAM-SCAR + rotations (– – –) formalism and the experimental electron TCSs from Możejko *et al* [5] (■).

4. Results and discussion

In table 1 and figure 2, we present the results of our positron-THFA total cross-section measurements. Note that the errors listed in table 1 and plotted in figure 2 are purely statistical and are at the one standard deviation level. Further note that the arrows in figure 2 indicate, respectively, the approximate thresholds for positronium formation (Ps) and the direct (first) ionization potential (IP) in THFA. It is known [32] that the first IP of THFA has a value of 9.43 ± 0.12 eV, leading to a positronium threshold value of 2.63 eV as in general:

$$E_{\mathrm{Ps}} = \mathrm{IP} - 6.8\,\mathrm{eV}. \tag{2}$$

In figure 2, we also plot the results of our present IAM-SCAR and IAM-SCAR + rotations computations, on the TCSs for electron scattering from THFA. These data are also tabulated in table 2. Finally, in figure 2, we provide the only available electron-THFA TCS measurement from Możejko *et al* [5].

Let us start by looking at the positron results, where it is clear (see figure 2) that as you go to lower positron energies the magnitude of the TCSs increases significantly (note the log-scale on the y-axis). This magnitude is even more significant when one considers the following two factors. Firstly, with an energy resolution $\sim$0.26 eV, our lowest energy TCSs ($\lesssim$0.5 eV) are actually a convolution over this energy width. In practice, this implies that when the TCSs are corrected for this effect they will somewhat further increase in magnitude. Secondly, the

Table 2. The present calculated TCSs ($\times 10^{-20}$ m^2) for electron scattering from THFA ($C_5H_{10}O_2$).

Energy (eV)	IAM-SCAR (10^{-20} m^2)	IAM-SCAR + rotational transitions (10^{-20} m^2)
1	97.7	282.8
1.5	91.3	221.2
2	84.8	185.6
3	73.1	143.1
4	67.8	121.8
5	64.1	108.4
7	59.1	91.8
10	54.0	77.6
15	50.7	66.9
20	49.3	61.9
30	47.0	55.7
40	44.5	51.2
50	42.0	47.3
70	38.1	42.0
100	33.6	36.4
150	28.6	30.5
200	25.0	26.5
300	20.2	21.3
400	17.1	17.9
500	14.9	15.6
700	11.9	12.4
1000	9.2	9.6
2000	5.4	5.5
3000	3.8	3.9
5000	2.5	2.5
10 000	1.3	1.4

data in table 1 are not corrected for forward angle scattering effects. Makochekanwa *et al* [33], using theoretical elastic DCSs, demonstrated that in water at 0.5 eV the TCS measured with their apparatus should be increased by ∼67% and at 5 eV by ∼53% to account for this effect. Similarly, now with formic acid, a 45% increase in the TCS for this effect at 4 eV positron energy was noted. As THFA has a larger dipole moment (and dipole polarizability) than either water or formic acid, it is reasonable to assume that this effect might even be more significant in THFA. Note that at higher positron energies, Makochekanwa *et al* [33] found that this correction was not as severe as at the lower energies. Further discussion of this effect can be found in Sullivan *et al* [19]. The low-energy behavior of the present positron-THFA total cross-section was not unexpected, as we have encountered similar trends in our previous work on polar biomolecules [8–10], [12, 13, 34], which we have ascribed to the strong dipole moments and significant dipole polarizabilities of those species. The present TCS shows a largely monotonic decrease in value with increasing the positron energy, until first the positronium channel, then the electronic-state channels and finally the direct ionization channel successively open. The

opening of these channels is usually seen as a small 'structure' or slope change in the measured TCSs.

Given our discussion above, the question 'Does this have any direct implications for cell damage at the molecular level?' should be addressed. Both the Berlin [35] and Innsbruck [36] groups have demonstrated with electrons that dissociative attachment at near-zero energies can be an important process, so that if positrons can similarly bind [37] it is conceivable that such large TCSs at epithermal energies might well have important implications in a fundamental understanding of positron emission tomography and positron 'needle' therapy processes, for example. This, however, remains speculative at this time. Notwithstanding, it is clear [38] that TCSs are fundamental inputs for particle track simulation codes, which incorporate realistic atomic and molecular data, with that application being an important rationale for this investigation.

The present IAM-SCAR and IAM-SCAR + rotations electron impact TCS calculation results are also plotted in figure 2, where they indicate the very important role played by the target dipole moment in the low-energy electron scattering dynamics. Interestingly, this effect becomes less pronounced as you go to higher energies, so that by about 100 eV (and thereafter) the two calculations are consistent with one another to better than $\sim$10%. While we would not, below 20 eV, expect our calculations to be exact, they nonetheless indicate the very large scattering cross-sections for this important biomolecule. In addition, the data listed in table 2 might be used as the starting parameters for energy deposition modelling in biologically relevant media and radiation damage research. Comparing the present IAM-SCAR + rotations TCS results with the measured electron-TCS data from Możejko *et al* [5] (see figure 2), we find rather good agreement between them for incident electron energies greater than about 30 eV. Below 30 eV, however, the theoretical and experimental results start to diverge. One reason for this is that the experimental results suggest the existence of two rather broad shape resonances which we believe are real and which our theory is incapable of reproducing. This represents a fundamental limitation of our IAM-SCAR formalism. In addition, below approximately 4 eV the experimental TCS magnitude continues to decrease with decreasing energy, while our theory TCS magnitude increases significantly with decreasing energy. In this case, however, we believe that the limitation lies in the experiment. Recall, in the context of our positron experiments, that we previously noted that the forward angle discrimination effect can significantly affect the TCS values at lower energies. This same effect is also germane to electron linear transmission TCS experiments, and as Możejko *et al* [5] do not correct for it, we believe that their lack of angular discrimination, at least in part, causes the discrepancy we observe, at the lower energies, in figure 2 between their measurements and our IAM-SCAR + rotations theory.

Comparing now our measured (positron) and calculated (electron) TCSs (again see figure 2), we observe that there is a qualitative correspondence between them at lower energies, i.e. a similar energy dependence for both leptons. Indeed, we are confident that this correspondence would become even more transparent once the forward angle scattering corrections are applied to the measured positron data. At higher energies the present positron TCSs appear to be tending towards our calculated electron TCSs, perhaps converging at around 200–300 eV. This we believe is physical, as the two most important phenomenological differences between them—exchange in the case of the incident electrons and positronium formation in the case of the incident positrons—both typically become small at incident projectile energies above 100 eV.

5. Conclusions

We have reported original total cross-section measurements and calculations for positron and electron scattering, respectively, from an important biomolecule, THFA. For both projectiles, the effect on the scattering dynamics at low energies of the target molecular dipole moment was significant. This was particularly well illustrated by the difference in the results of our IAM-SCAR and IAM-SCAR + rotations computations. Good agreement between our IAM-SCAR + rotations results and the electron TCS measurements of Możejko *et al* was also noted for incident electron energies greater than about 30 eV.

Acknowledgments

This work was supported under a Memorandum of Understanding between the University of Trento and the Flinders University node of the ARC Centre for Antimatter-Matter Studies. GG and FB thank the Spanish Ministerio de Ciencia e Innovacion (project no. FIS2009–10245) and the EU Famework Programme (COST Action MP1002).

References

[1] Fuss M C, Muñoz A, Oller J C, Blanco F, Hubin-Franskin M-J, Almeida D, Limão-Vieira P and García G 2010 *Chem. Phys. Lett.* **486** 110
[2] Muñoz A, Blanco F, García G, Thorn P A, Brunger M J, Sullivan J P and Buckman S J 2008 *Int. J. Mass Spectrom.* **277** 175
[3] Milosavljević A R, Blanco F, Sević D, Garcia G and Marinković B P 2006 *Eur. Phys. J.* D **40** 107
[4] Szmytkowski C and Ptasińska-Denga E 2011 *J. Phys. B: At. Mol. Opt. Phys.* **44** 015203
[5] Możejko P, Domaracka A, Ptasińska-Denga E and Szmytkowski C 2006 *Chem. Phys. Lett.* **429** 378
[6] Chiari L, Brunger M J and Zecca A 2011 *Radiation Damage in Biomolecular Systems* ed G García (Berlin: Springer)
[7] Kato H *et al* 2010 *J. Chem. Phys.* **132** 074309
[8] Zecca A, Sanyal D, Chakrabarti M and Brunger M J 2006 *J. Phys. B: At. Mol. Opt. Phys.* **39** 1597
[9] Zecca A, Perazzolli C and Brunger M J 2005 *J. Phys. B: At. Mol. Opt. Phys.* **38** 2079
[10] Zecca A, Chiari L, Sarkar A and Brunger M J 2008 *J. Phys. B: At. Mol. Opt. Phys.* **41** 085201
[11] Zecca A, Chiari L, Nixon K L, Brunger M J, Chattopadhyay S, Sanyal D and Chakrabarti M 2009 *J. Phys. Chem.* A **113** 14251
[12] Zecca A, Chiari L, Trainotti E, Sarkar A and Brunger M J 2010 *PMC Phys.* B **3** 4
[13] Zecca A, Chiari L, Garcia G, Blanco F, Trainotti E and Brunger M J 2010 *J. Phys. B: At. Mol. Opt. Phys.* **43** 215204
[14] Zecca A, Chiari L, Sarkar A, Chattopadhyay S and Brunger M J 2010 *Nucl. Instrum. Methods* B **268** 533
[15] Jones A C L, Makochekanwa C, Caradonna P, Machacek J R, McEachran R P, Sullivan J P, Buckman S J, Stauffer A D, Bray I and Fursa D V 2011 *Phys. Rev.* A **83** 032701
[16] Makochekanwa C 2010 private communication
[17] Kauppila W E, Stein T S, Smart J H, Dababneh M S, Ho Y K, Downing J P and Pol V 1981 *Phys. Rev.* A **24** 725
[18] Hamada A and Sueoka O 1994 *J. Phys. B: At. Mol. Opt. Phys.* **27** 5055
[19] Sullivan J P, Makochekanwa C, Jones A, Caradonna P, Slaughter D S, Machacek J, McEachran R P, Mueller D W and Buckman S J 2011 *J. Phys. B: At. Mol. Opt. Phys.* **44** 035201
[20] Zecca A and Brunger M J 2007 *Nanoscale Interactions and Their Applications: Essays in Honour of Ian McCarthy* ed F Wang and M J Brunger (Trivandrum: Research Signpost)

[21] Takaishi T and Sensui Y 1963 *Trans. Faraday Soc.* **59** 2503
[22] Cowan R D 1981 *The Theory of Atomic Structure and Spectra* (London: University of California Press)
[23] Riley M E and Truhlar D G 1975 *J. Chem. Phys.* **63** 2182
[24] Zhang X Z, Sun J F and Liu Y F 1992 *J. Phys. B: At. Mol. Opt. Phys.* **25** 1893
[25] Staszewska G, Schwenke D W, Thirumalai D and Truhlar D G 1983 *Phys. Rev.* A **28** 2740
[26] Blanco F and García G 2002 *Phys. Lett.* A **295** 178
[27] Blanco F and García G 2003 *Phys. Rev.* A **67** 022701
[28] Zatsarinny O *et al* 2011 *Phys. Rev.* A **83** 042702
[29] Maljković J B, Milosavljević A R, Blanco F, Šević D, García G and Marinković B P 2009 *Phys. Rev.* A **79** 052706
[30] Blanco F and Garcia G 2004 *Phys. Lett.* A **330** 230
[31] Blanco F and García G 2009 *J. Phys. B: At. Mol. Opt. Phys.* **42** 145203
[32] Milosavljević A R, Kocisek J, Papp P, Kubala D, Marinković B P, Mach R, Urban J and Matejcik S 2010 *J. Chem. Phys.* **132** 104308
[33] Makochekanwa C *et al* 2009 *New J. Phys.* **11** 103036
[34] Zecca A, Chiari L, Sarkar A, Lima M A P, Bettega M H F, Nixon K L and Brunger M J 2008 *Phys. Rev.* A **78** 042707
[35] Hamel G, Gstir B, Denifl S, Scheier P, Probst M, Farizon B, Farizon M, Illenberger E and Märk T D 2003 *Phys. Rev. Lett.* **90** 188104
[36] Sulzer P *et al* 2006 *J. Chem. Phys.* **125** 044304
[37] Danielson J R, Gosselin J J and Surko C M 2010 *Phys. Rev. Lett.* **104** 233201
[38] Sanz A G, Fuss M C, Roldán A M, Blanco F, Limão-Vieira P, Brunger M J, Buckman S J and García G 2011 *Int. J. Radiat. Biol.* submitted